

RSC Advances



This is an *Accepted Manuscript*, which has been through the Royal Society of Chemistry peer review process and has been accepted for publication.

Accepted Manuscripts are published online shortly after acceptance, before technical editing, formatting and proof reading. Using this free service, authors can make their results available to the community, in citable form, before we publish the edited article. This *Accepted Manuscript* will be replaced by the edited, formatted and paginated article as soon as this is available.

You can find more information about *Accepted Manuscripts* in the [Information for Authors](#).

Please note that technical editing may introduce minor changes to the text and/or graphics, which may alter content. The journal's standard [Terms & Conditions](#) and the [Ethical guidelines](#) still apply. In no event shall the Royal Society of Chemistry be held responsible for any errors or omissions in this *Accepted Manuscript* or any consequences arising from the use of any information it contains.

The Stability, Electronic Properties, and hardness of SiN₂ under High Pressure

Changbo Chen^{a,*}, Ying Xu^a, Xiuping Sun^a, Sihang Wang^a, Fubo Tian^b

^a School of Science, Changchun University of Science and Technology, Changchun 130022, P. R. China.

^b State Key Laboratory of Superhard Materials, College of physics, Jilin University, Changchun, 130012, P. R. China.

Abstract

The structures of silicon nitride (SiN₂) under high pressures have been predicted using the developed particle swarm optimization algorithm for crystal structure prediction. The pyrite SiN₂ can be synthesized above 17 GPa, and the current thermodynamical calculations reveal that the pyrite-type structure is the most stable up to 100 GPa. No imaginary phonon frequencies in the whole Brillouin zone indicate the pyrite SiN₂ is dynamically stable. Strickingly, the mechanical analyses show the Pyrite SiN₂ displays a behavior very similar to isotropy and high bulk modulus, shear modulus, and high simulated hardness indicate its very incompressible and superhard nature (63 GPa), which was driven by the strong covalent Si–N bonds and localized nonbonding.

Introduction

Superhard materials are of great importance due to the science and technology applications such as scratch-resistant coatings to polishing and cutting tools, etc¹⁻³. Extensive experiments and theoretical work have been performed with a focus on searching novel superhard materials and understanding the properties of those. Light elements e.g., boron, carbon, nitrogen, and oxygen can form the strong covalent compounds⁴⁻⁶ which can withstand both elastic and plastic deformations. Moreover, pressure can also be seen an effective tools for increasing the density of materials and altering the electronic bonding states to induce the formation of the new superhard materials or modify the physical properties⁷. With the ideas, designing the novel superhard materials under high pressure is a scientific and effective way.

The triple $\text{N}\equiv\text{N}$ bond in nitrogen is the strongest bond known, however, the triple bonded molecular collapses to form $\text{N}-\text{N}$ bond at moderate pressures⁸⁻¹⁰, which can help to form new nitrides with other elements, moreover, these nitrides such as silicon nitrides have the novel physical properties. Si_3N_4 is an important ceramic with many diverse applications, especially, in high temperature and corrosive environment. Up to now, there are three stable phases of Si_3N_4 with the trigonal(α - Si_3N_4), hexagonal(β - Si_3N_4), and cubic(γ - Si_3N_4) phases¹¹⁻¹³. The

theoretical calculations showed that the β - Si_3N_4 phase was more stable than the α - Si_3N_4 phase at 0 K. Under high pressure and high temperature, the α - Si_3N_4 and β - Si_3N_4 can transform into γ - Si_3N_4 . As far as silicon nitrides, the other form is SiN_2 , which is considered as a pyrite-type structure with a space group of $Pa-3$ that is consistent with CN_2 and GeN_2 ¹⁴. Recently, the first principle studies¹⁵ have showed that *bct*- CN_2 is energetically much superior to previously proposed pyrite structure under high pressures and *bct*- CN_2 has high calculated ideal strength, bulk modulus, shear modulus, and simulated hardness. However, the structures of SiN_2 under high pressure are unclear, which are well worthy exploring, moreover, the stability, electronic properties, and hardness of SiN_2 under high pressure are the objects of our researches.

In this paper, we have predicted the structures of SiN_2 under high pressures by recently developed particle swarm optimization (PSO) algorithm¹⁶⁻²³ on crystal structural prediction. The pyrite SiN_2 can be synthesized above 17 GPa, and the current thermodynamical calculations reveal that the pyrite-type structure is the most stable up to 100 GPa. The electronic calculations indicate the pyrite SiN_2 is insulator by the energy band gap 5.13 eV, and the strong covalent bonds are formed by the hybridizations between Si and N electrons. For further understanding the mechanical properties, the anisotropy, high bulk modulus, high shear modulus, and high simulated hardness are uncovered, which indicate its

very incompressible and superhard nature (63 GPa), which was driven by the strong covalent Si–N bonds and localized nonbonding.

Computational methods

Searches for candidate high-pressure structures (0-100 GPa) of SiN₂ are performed using the variable-cell PSO simulations¹⁶⁻²³ with the CALYPSO code²⁰ developed for crystal-structure prediction and up to 12 atoms in the unit cell. The underlying *ab initio* structure relaxations are performed using density functional theory^{24, 25} within the Perdew-Burke-Ernzerhof (PBE) parameterization of the generalized gradient approximation (GGA)²⁶ as implemented in the Vienna *ab initio* simulation package VASP code²⁷. The all-electron projector-augmented wave (PAW)²⁸ method is adopted with the choices of 3s²3p² and 2s²2p³ cores for Si and N atoms, respectively. The plane-wave kinetic energy cutoff of 800 eV and a k-mesh of 0.03 Å⁻¹ grid spacing within the Monkhorst-Pack scheme²⁹ for sample the Brillouin zone are used, which give an excellent convergence of the total energies, energy differences, and structural parameters. In order to obtain the elastic properties, *ab initio* pseudopotential plane-wave density functional method implemented in the CASTEP code³⁰ has been used. Exchange and correlation effects are described in the scheme of Perdew-Burke-Ernzerhof of GGA²⁶. Vanderbilt ultrasoft pseudopotentials³¹ were generated for Si and N with the valence configuration of 3s²3p²

and $2s^22p^3$, respectively. The cutoff energy and k-mesh are same as the setting in VASP calculations. The phonon frequencies are calculated using direct supercell method³² with the PHONOPY code³³.

Results and discussion

Searches of the structures within 2, 3 and 4 formula units (f.u.) are performed in the pressure range of 0-100 GPa by using the pso method. Analysis of the predicted structures give us a shortlist of candidate structures with space groups *Pa-3* (4 f.u. per cell), *C2m* (6 f.u. per cell), *Cmc2₁* (4 f.u. per cell), *Pnma* (4 f.u. per cell), *P6₃/mmc* (2 f.u. per cell), and *R-3m* (3 f.u. per cell), as schematically shown in Fig. 1. *Pa-3* structure (pyrite structure) predicted here is the same as the structure proposed by Wehrich et al.¹⁴ using a substitution method with the knowledge of isoelectronic SiP₂ structure. Si atoms occupy the center of the Octahedral and one Si atom bonds to six N atoms forming SiN₆ cluster. The other five structures reported here for the first time have N-N bonds that are different from pyrite-type structure. The structural details of the lattice parameters and the atomic positions are listed in Table. For further investigating the stability of the structures, the thermodynamic stability of the various predicted structures need to calculate the formation enthalpies at a large pressure range from 0 to 100 GPa according to the reaction:

$$\Delta H = H_{SiN_2} - \frac{1}{3}(H_{Si_3N_4} + H_{N_2})$$

To get a more realistic prediction, both the experimental³⁴ and computational^{35, 36} high-pressure (low temperature) phase orders of nitrogen were adopted. The α -Si₃N₄, and β -Si₃N₄ was chosen as the reference phases in our calculations. Fig. 2 shows the curves of the formation enthalpy for the predicted structures at high pressures. Pyrite SiN₂ can be formed at 17 GPa and becomes the most stable phase until 100 GPa.

It is of fundamental importance to check the phonon spectra of the Pyrite SiN₂ due to its providing the information of the structural stability. The calculations of the phonon frequencies are performed at 0 GPa and 20 GPa, respectively. The phonon dispersion curves along the high symmetry direction are shown in Fig. 3. It is clear that no imaginary phonon frequency exists in the whole BZ, indicating the dynamical stability of the phase. As the pressure increases, all modes shift to higher frequencies. The results show that Pyrite SiN₂ will be dynamically stable up to 100 GPa.

The calculations of the elastic constants are essential, which can help to investigate the mechanical properties of the materials that are important in the industry applications, and also to be regarded as the mechanical stability criteria³⁷. The elastic constants C_{ij} of the Pyrite SiN₂ have been calculated using the CASTEP code and are listed as the

following: $C_{11} = 704$ GPa, $C_{44} = 379$ GPa, $C_{12} = 127$ GPa, which satisfy the mechanical criteria: $C_{11} > 0$, $C_{44} > 0$, $C_{11} > |C_{12}|$, and $(C_{11} + 2|C_{12}|) > 0$. The elastic anisotropy factors³⁸ providing the convenient measure of in-plane phonon focusing are studied for the Pyrite SiN_2 . $C_L = C_{44} + (C_{11} + C_{12})/2 = 794.5$ GPa; $A_{100} = 2C_{44}/(C_{11} - C_{12}) = 1.31$; $A_{110} = C_{44}(C_L + 2C_{12} + C_{11})/(C_L C_{11} - C_{12}^2) = 1.22$. It is found that the elastic anisotropy for the [100] planes is close to that for the [110] planes. Poisson's ratio (ν) provides important information about the characteristics of the bonding forces; for example, it characterizes the stability of the crystal against shearing strain. Our results show that the Poisson's ratio of the Pyrite SiN_2 is 0.15. Due to such a low Poisson's ratio, the Pyrite-type SiN_2 would be isotropic. The elastic anisotropy can be represented by the Young's modulus on a direction in a crystal³⁹. For the cubic materials, it can be described by the following equation:

$$E^{-1} = s_{11} - \beta_1 (\alpha^2 \beta^2 + \alpha^2 \gamma^2 + \beta^2 \gamma^2)$$

Where α , β , and γ are the direction cosines of the tensile stress direction, $\beta_1 = 2s_{11} - 2s_{12} - s_{44} < 0$, and s_{11} , s_{12} , and s_{44} , are the elastic compliance constants. The elements of the matrix representation of tensor s have the relationships with those of the matrix representation of tensor C in Voigt's contracted notation as follows: $s_{11} = (C_{11} - C_{12}) / (C_{11}^2 + C_{11}C_{12} - 2C_{12}^2) = 1.044 \times 10^{-3} \text{ GPa}^{-1}$, $s_{12} = C_{12} / (C_{11}^2 + C_{11}C_{12} - 2C_{12}^2) = 2.3 \times 10^{-4} \text{ GPa}^{-1}$, and $s_{44} = 1/C_{44} = 2.600 \times 10^{-3} \text{ GPa}^{-1}$. From the elastic compliance

constants above we can get $\beta_1=9.7\times 10^{-3}$ GPa⁻¹, which is very close to zero indicating the Pyrite SiN₂ display a behavior very similar to isotropy, that is consistent with the calculated Poisson's ratio.

The calculated bulk modulus can reach 320 GPa, which imply the Pyrite SiN₂ is an ultra-incompressible material. The shear modulus is 343 GPa estimated by using the Wu's results³⁷, that can resist to the reversible deformation under shear strain and provide the proofs for the superhardness. The simulated hardness of the Pyrite SiN₂ is 63GPa calculated with the model by Xing-Qiu Chen et al.⁴⁰, which is closed to c-BN (66 GPa) and BC₅ (71 GPa) indicating Pyrite SiN₂ is a superhard material. In order to better understand the origin of the superhardness, we examine the electronic band structure, electronic partial density of states, and electron localization functions (ELFs). The electronic band and partial density of states calculations indicate the pyrite SiN₂ is insulator by the energy band gap 5.13 eV as plotted in Fig. 4 (a) and Fig. 4 (b). The ELFs provide the information for distinguishing the ionic, metallic, and covalent bonding. High ELF (≥ 0.8) indicates the formation of covalent bonds. Fig. 4 (c) shows the isosurface of ELF=0.88, it is clear that one Si atom bonds to six N atoms and form the strong covalent directional bonds. The electronic partial density of states is depicted by Fig. 4 (b) and characterizes two aspects: One is that the strong covalent directional bonds are formed by the hybridizations between Si *s, p* electrons and N *s,*

p electrons. The other is the excess electrons of N p electrons in the energy range of -10 eV and 0 eV cannot form the covalent bonds, but form stable and localized non-bonded states, which share the same properties as *bct*-CN₂. The strong covalent Si–N bonds and localized nonbonding are responsible for its high bulk shear modulus and simulated hardness at equilibrium.

Conclusion

In summary, the structures of silicon nitride (SiN₂) under high pressures have been predicted using the developed particle swarm optimization algorithm for crystal structure prediction. The pyrite SiN₂ can be synthesized above 17 GPa, and the current thermodynamical calculations reveal that the pyrite-type structure is the most stable up to 100 GPa. No imaginary phonon frequencies in the whole Brillouin zone indicate the pyrite SiN₂ is dynamically stable. The electronic calculations show the pyrite SiN₂ is insulator by the energy band gap 5.13 eV, and the strong covalent bonds are formed by the hybridizations between Si and N electrons. Strikingly, the mechanical analyses show the pyrite SiN₂ display a behavior very similar to isotropy and high bulk modulus, shear modulus, and high simulated hardness indicate its very incompressible and superhard nature, which was driven by the strong covalent Si–N bonds and localized nonbonding. We believe that the current study will

contribute to the experimental synthesis and determination of silicon nitrides and understanding the novel properties of the materials.

Acknowledgements

This work was supported by the the National Natural Science Foundation of China (Nos. 11104019, 11104102). Parts of calculations were performed in the Scientific Computation and Numerical Simulation Center of Changchun University of Science and Technology.

Reference:

*Author to whom correspondence should be addressed:

chencb@cust.edu.cn

1. A. G. Thornton and J. Wilks, *Nature*, 1978, 274, 792.
2. R. B. Kaner, J. J. Gilman and S. H. Tolbert, *Science*, 2005, 308, 1268.
3. V. L. Solozhenko, D. Andrault, G. Fiquet, M. Mezouar and D. C. Rubie, *Appl. Phys. Lett.*, 2001, 78, 1385.
4. X. Hao, Y. Xu, Z. Wu, D. Zhou, X. Liu and J. Meng, *J. Alloys Compounds.*, 2008, 453, 413.
5. F. Tian, J. Wang, Z. He, Y. Ma, L. Wang, T. Cui, C. Chen, B. Liu and G. Zou, *Phys. Rev. B*, 2008, 78, 235431.
6. Z. Wang, Y. Zhao, P. Lazor, H. Annersten and S. K. Saxena, *Appl. Phys. Lett.*, 2005, 86, 041911.
7. Z. Zhao, K. Bao, D. Li, D. Duan, F. Tian, X. Jin, C. Chen, X. Huang, B. Liu and T. Cui, *Sci. Rep.*, 2014, 4, 04797.
8. W. J. Nellis, N. C. Holmes, A. C. Mitchell and M. van Thiel, *Phys. Rev. Lett.*, 1984, 53, 1661.
9. M. I. Eremets, R. J. Hemley, H.-k. Mao and E. Gregoryanz, *Nature*, 2001, 411, 170.
10. Y. Ma, A. R. Oganov, Z. Li, Y. Xie and J. Kotakoski, *Phys. Rev. Lett.*, 2009, 102, 065501.
11. W.-Y. Ching, Y.-N. Xu, J. D. Gale and M. Rühle, *J. Am. Ceram. Soc.*,

1998, 81, 3189.

12. C. Dong and Y. Ben-Hai, *Chin. Phys. B*, 2013, 22, 023104.

13. A. Mirgorodsky, M. Baraton and P. Quintard, *Phys. Rev. B*, 1993, 48, 13326.

14. R. Weihrich, V. Eyert and S. F. Matar, *Chem. Phys. Lett.*, 2003, 373, 636.

15. Q. Li, H. Liu, D. Zhou, W. Zheng, Z. Wu and Y. Ma, *Phys. Chem. Chem. Phys.*, 2012, 14, 13081.

16. L. Zhu, Z. Wang, Y. Wang, G. Zou, H.-k. Mao and Y. Ma, *PNS*, 2012, 109, 751.

17. H. Liu, Q. Li, L. Zhu and Y. Ma, *Phys. Lett. A*, 2011, 375, 771.

18. P. Li, G. Gao, Y. Wang and Y. Ma, *J. Phys. Chem. C*, 2010, 114, 21745.

19. Y. Wang, J. Lv, L. Zhu and Y. Ma, *Phys. Rev. B*, 2010, 82, 094116.

20. Y. Wang, M. Miao, J. Lv, L. Zhu, K. Yin, H. Liu and Y. Ma, *J. Chem. Phys.*, 2012, 137, 224108.

21. G. Gao, H. Wang, L. Zhu and Y. Ma, *J. Phys. Chem. C*, 2011, 116, 1995.

22. H. Wang, J. S. Tse, K. Tanaka, T. Iitaka and Y. Ma, *PNAS*, 2012, 109, 6463.

23. Y. Wang, H. Liu, J. Lv, L. Zhu, H. Wang and Y. Ma, *Nat Commun*, 2011, 2, 563.

24. S. Baroni, P. Giannozzi and A. Testa, *Phys. Rev. Lett.*, 1987, 58, 1861.
25. P. Giannozzi, S. De Gironcoli, P. Pavone and S. Baroni, *Phys. Rev. B*, 1991, 43, 7231.
26. J. P. Perdew, K. Burke and M. Ernzerhof, *Phys. Rev. Lett.*, 1996, 77, 3865.
27. G. Kresse and J. Furthmüller, *Phys. Rev. B*, 1996, 54, 11169.
28. P. E. Blöchl, *Phys. Rev. B*, 1994, 50, 17953.
29. H. J. Monkhorst and J. D. Pack, *Phys. Rev. B*, 1976, 13, 5188.
30. M. Segall, P. J. Lindan, M. Probert, C. Pickard, P. Hasnip, S. Clark and M. Payne, *J. Phys.: Condens. Matter*, 2002, 14, 2717.
31. D. Vanderbilt, *Phys. Rev. B*, 1990, 41, 7892.
32. K. Parlinski, Z. Li and Y. Kawazoe, *Phys. Rev. Lett.*, 1997, 78, 4063.
33. A. Togo, F. Oba and I. Tanaka, *Phys. Rev. B*, 2008, 78, 134106.
34. E. Gregoryanz, A. F. Goncharov, C. Sanloup, M. Somayazulu, H.-k. Mao and R. J. Hemley, *J. Chem. Phys.*, 2007, 126, 184505.
35. C. J. Pickard and R. J. Needs, *Phys. Rev. Lett.*, 2009, 102, 125702.
36. X. Wang, Y. Wang, M. Miao, X. Zhong, J. Lv, T. Cui, J. Li, L. Chen, C. J. Pickard and Y. Ma, *Phys. Rev. Lett.*, 2012, 109, 175502.
37. Z.-j. Wu, E.-j. Zhao, H.-p. Xiang, X.-f. Hao, X.-j. Liu and J. Meng, *Phys. Rev. B*, 2007, 76, 054115.
38. K. Lau and A. K. McCurdy, *Phys. Rev. B*, 1998, 58, 8980.
39. A. Cazzani and M. Rovati, *International J. Solids Struct.*, 2003, 40,

1713.

40. X.-Q. Chen, H. Niu, D. Li and Y. Li, *Intermetallics*, 2011, 19, 1275.

Caption:

Fig. 1. Crystal structures of competing SiN_2 phases at 0-100 GPa

Fig. 2. The enthalpy curves relative to $\text{Si}_3\text{N}_4+\text{N}_2$ as a function of pressure

Fig. 3. The phonon dispersion curves for Pyrite SiN_2 . (a) at 0 GPa and (b) at 20 GPa

Fig. 4. (a) The electronic band structure at 0 GPa (b) the electronic partial density of states at 0 GPa (c) the electron localization functions (ELFs) at 0 GPa

Table. Predicted lattice constants and atomic coordinates, as referred to the conventional unit cells, of the predicted structures at 0 GPa

Table

space group	lattice parameter (Å)	atomic coordinates (fractional)
<i>Pa-3</i>	a=4.455	Si 4b (0.5, 0, 0)
		N 8c (0.4049, 0.9048, 0.5951)
<i>Pnma</i>	a=7.181, b=2.823,	Si 4c (0.3731, 0.25, 0.3174)
	c=4.491	N 4c (0.7942, 0.25, 0.5788)
		N 4c (0.9547, 0.25, 0.7797)
<i>C2/m</i>	a=10.254, b=2.824,	Si 2c (0, 0, 0.5)
	c=9.051, $\beta=144.8$	Si 4i (0.5543, 0, 8261)
		N 4i (0.3365, 0, 0.4424)
		N 4i (0.8870, 0, 0.7461)
		N 4i (0.8173, 0, 0.1688)
<i>P6₃/mmc</i>	a=2.809, c=6.764	Si 2a (0, 0, 0)
		N 4f (0.6667, 0.3331, 0.6418)
<i>Cmc2₁</i>	a=2.906, b=7.487	Si 4a (0, 0.8566, 0.1686)
	c=4.548	N 4a (0, 0.9327, 0.5367)
		N 4a (0, 0.7839, 0.7410)
<i>R-3m</i>	a=4.716, $\alpha=108.8$	Si 3d (0.5, 0, 0)
(Rhombohedral representation)		N 6h (0.6563, 0.6563, 0.0391)

Fig1

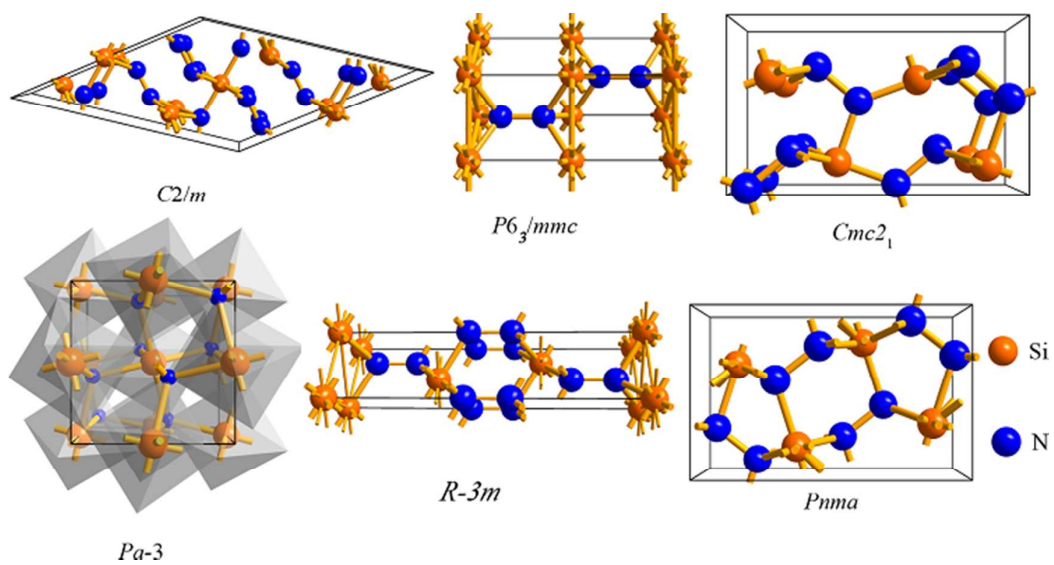


Fig 2

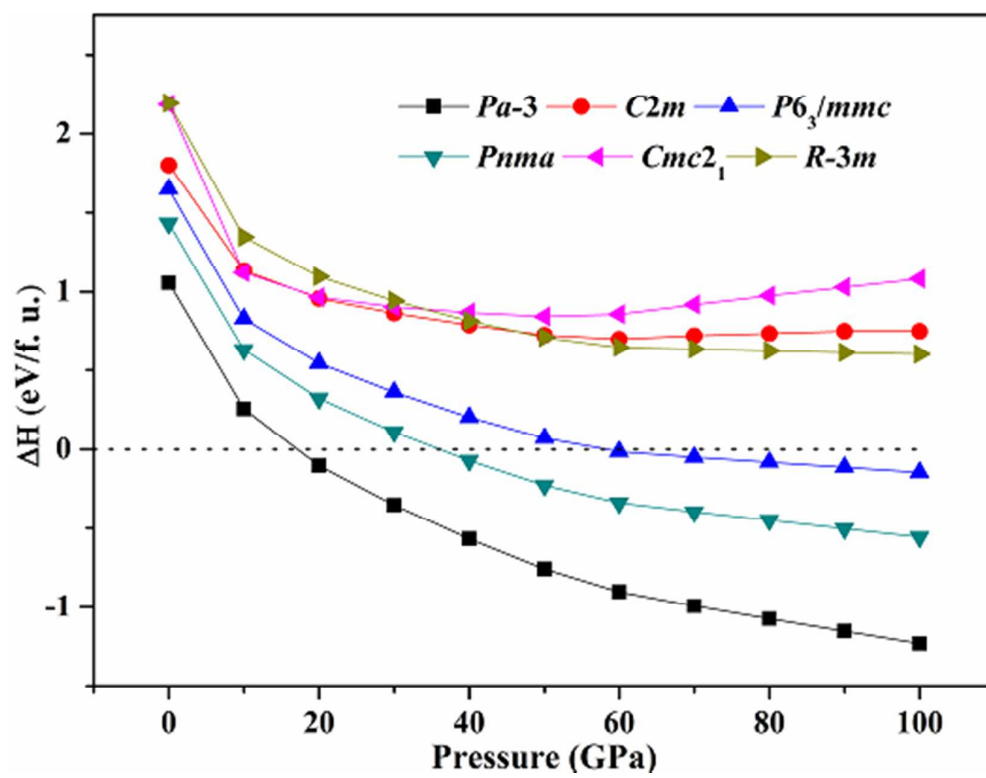


Fig3

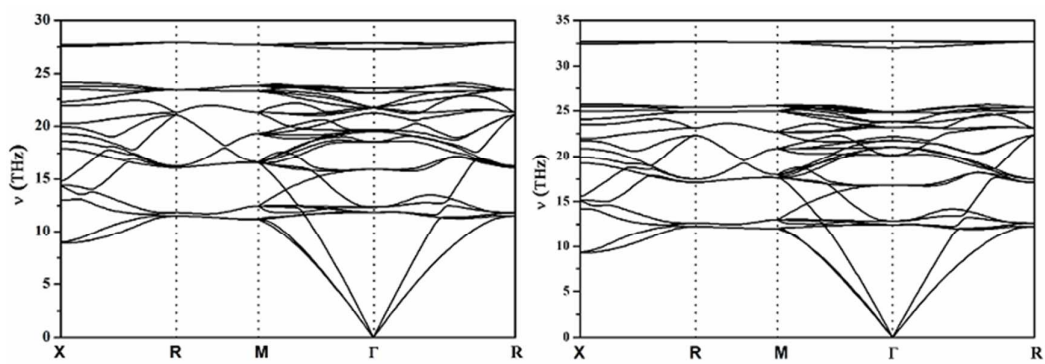
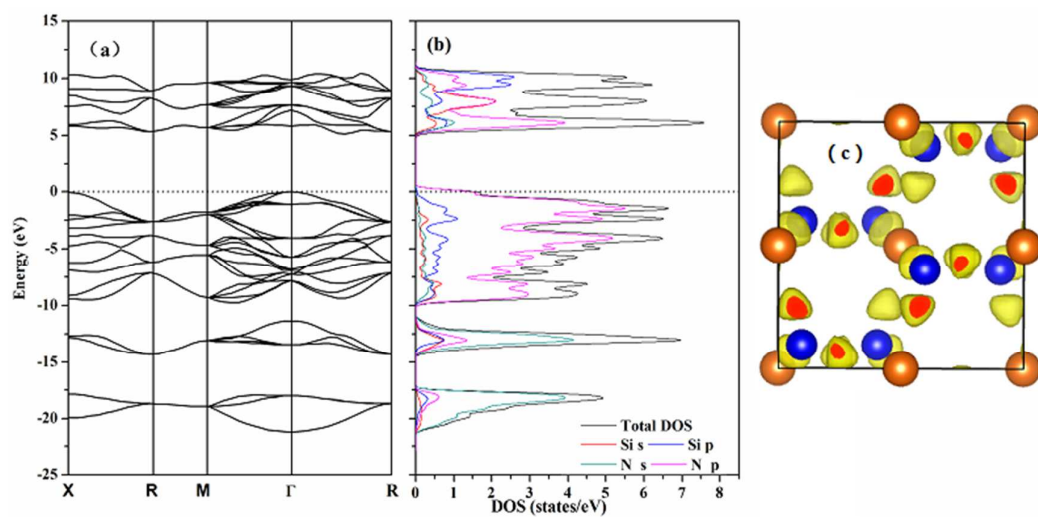


Fig4

**Highlight:**

Pyrite SiN_2 displays a behavior very similar to isotropy and high simulated hardness (63 GPa).